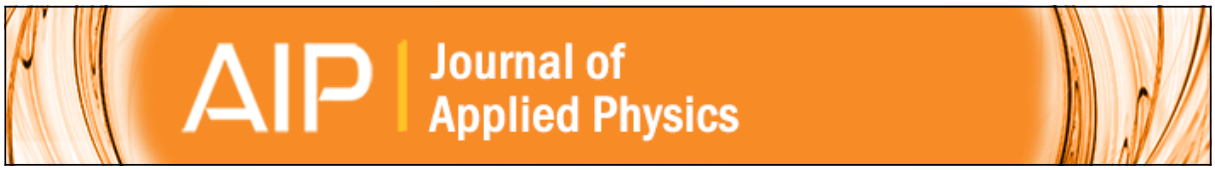

Deep states in GaAs grown by molecular beam epitaxy

P. Blood and J. J. Harris

Citation: Journal of Applied Physics **56**, 993 (1984); doi: 10.1063/1.334040
View online: http://dx.doi.org/10.1063/1.334040
View Table of Contents: http://scitation.aip.org/content/aip/journal/jap/56/4?ver=pdfcov
Published by the AIP Publishing

Articles you may be interested in

Annealing effect on concentration of EL6-like deep-level state in low-temperature-grown molecular beam epitaxial GaAs
Appl. Phys. Lett. **72**, 590 (1998); 10.1063/1.120815

Deep levels in GaAs grown by atomic layer molecular beam epitaxy
Appl. Phys. Lett. **65**, 2848 (1994); 10.1063/1.112512

Deep traps in molecularbeamepitaxial GaAs grown at low temperatures
J. Appl. Phys. **76**, 1029 (1994); 10.1063/1.357846

Deep states and misfit dislocations in indiumdoped GaAs layers grown by molecular beam epitaxy
Appl. Phys. Lett. **52**, 2258 (1988); 10.1063/1.99530

Relation between growth conditions and deep levels in GaAs grown by molecularbeam epitaxy
J. Appl. Phys. **62**, 2136 (1987); 10.1063/1.339509

[This article is copyrighted as indicated in the article. Reuse of AIP content is subject to the terms at: http://scitation.aip.org/termsconditions. Downloaded to] IP: 133.1.198.126 On: Wed, 26 Nov 2014 07:07:39

Deep states in GaAs grown by molecular beam epitaxy

P. Blood and J. J. Harris
Philips Research Laboratories, Redhill, Surrey RH1 5HA, England

(Received 18 January 1984; accepted for publication 14 March 1984)

Using deep level transient capacitance spectroscopy (DLTS) we have investigated the growth parameter dependence and electronic properties of deep level centers in GaAs grown by molecular beam epitaxy (MBE), principally in the temperature range 500–650 °C. In both *n*- and *p*-type material we find hole traps ascribed to Fe and Cu and electron traps *M* 1, *M* 3 and *M* 4 unique to MBE layers. Concentrations of the "*M*" levels depend weakly on As:Ga flux ratio but decrease rapidly with increasing growth temperature. Depth profiles show no evidence for bulk annealing and, by comparison with published secondary ion mass spectrometry data, we suggest these centers are impurity-defect complexes. Capture cross-section (σ_n) measurements show that two different traps give rise to further DLTS peaks at ~140 K. One trap with $\sigma_n > 4\times10^{-17}$ cm^2 and $(E_c - E_t) > 0.17$ eV (at 140 K), which we associate with *M* 2, is observed at a growth temperature of 650 °C and from the influence of the growth conditions we suggest this is As-vacancy related. The other trap, which we label *M* 2′, has $\sigma_n = 1\times10^{-20}$ cm^2 and $(E_c - E_t) = 0.08$ eV (at 140 K) and occurs in material grown at temperatures below 600 °C, with similar growth behavior to *M* 1, *M* 3 and *M* 4. For *M* 3 we measured $\sigma_n = 1.1\times10^{-16}$ cm^2 giving $(E_c - E_t) = 0.23_6$ eV at 173 K. Using measurements of the temperature dependence of σ_n we have calculated the entropy change on emission or capture of an electron at *M* 2′ and *M* 3 and deduce that these levels are associated with bonding (valence band) states. The capture cross sections of *M* 1 and *M* 4 were too large to be measured ($> 2\times10^{-16}$ cm^2), but we deduce that $\sigma_n(M4) > \sigma_n(M1)$. Data are given for the signatures of all the electron traps at low electric fields, and these are compared with data for other traps in GaAs. We do not find convincing evidence for identifying the DLTS peak at 200 K in 300 °C grown material with the *E* 3 center in irradiated GaAs. We suggest that the minority carrier lifetime in *p*-GaAs will be limited by recombination at *M* 4 and *M* 2 for growth temperatures below and above ~625 °C, respectively.

I. INTRODUCTION

Despite many years of research, very little is known concerning the nature of the centers which give rise to the wide variety of deep states observed electrically in GaAs. Although the study of deep states introduced by intentional irradiation shows some promise, this approach does not address the important problem of the origin of deep states in as-grown material, particularly thin epitaxial layers. Here the principal method of investigation has been concerned with the influence of growth conditions, though often there is not sufficient understanding of the growth mechanisms involved to enable the growth conditions to be related to the formation and incorporation of defects and impurities in the growing crystal.

Molecular beam epitaxy (MBE) is now an established technique for the growth of thin GaAs films. The surface processes controlling the growth mechanism in MBE have been studied in considerable detail[1] and growth conditions can be monitored by measuring parameters such as the molecular flux and substrate temperature. MBE material therefore offers the prospect of a more fruitful study of the occurrence of growth related deep states than the older processes such as liquid phase epitaxy (LPE) and vapor phase epitaxy (VPE). In the device area, MBE is being used with particular success in the preparation of optoelectronic devices. The efficiency of such devices may be degraded by nonradiative recombination via deep states and so knowledge of deep states in this material is of practical importance.

The first study of deep states in *n*-GaAs grown by MBE was reported by Lang *et al.*[2]; using transient capacitance measurements (DLTS), they observed nine different electron traps, labelled *M* 0....*M* 8. The conclusion was that these traps are characteristic of the growth process which implies that the occurrence of these levels should be influenced by the growth conditions. This has been borne out by later brief reports of the effect of changing the growth temperature[3] and the effect of the arsenic species, As_2 or As_4.[4]

As a result of improvements in the design of MBE growth systems and greater operational experience it is now possible to produce high-purity layers with good reproducibility. This has encouraged us to undertake more detailed investigations than hitherto on the effect of growth temperature and As:Ga ratio on the deep states in *n*-type MBE GaAs using both Si and Sn as dopants.

The electronic properties of deep states observed in different samples are usually compared by means of Arrhenius plots of the temperature dependence of the emission rate. As a working hypothesis it is assumed that levels with the same "signature" are due to the same kind of center. This procedure may be jeopardized by enhancement of the emission rate by the electric field present in the depletion region of the DLTS sample. No information on the electric field was given by Lang *et al.*[2] for their diodes but the doping levels in their material (10^{16} cm$^{-3} < n < 2\times10^{17}$ cm^{-3} for all but one sample) suggest the fields could have been large. We have recorded data for the emission rates as a function of temperature for

 0021-8979/84/160993-15$02.40 © 1984 American Institute of Physics

[This article is copyrighted as indicated in the article. Reuse of AIP content is subject to the terms at: http://scitation.aip.org/termsconditions. Downloaded to] IP: 133.1.198.126 On: Wed, 26 Nov 2014 07:07:39

the principal electron traps in MBE GaAs using lower doped samples and with low applied voltages such that the emission rates were not enhanced by the field. We have also obtained new emission rate data for trap $M2$ and have examined the signature of the dominant trap in low-temperature (300 °C) grown material for the first time.

The capture cross sections are of interest because they control the recombination rate at the trap and provide a further property which can be used to identify deep level centers. We have measured the capture cross section for $M3$ and for the DLTS peak at 140 K in the position assigned to $M2$. We conclude there are two 140 K traps with different cross sections, occurring at different growth temperatures, with similar signatures. One trap corresponds to $M2$,[2] the other we label $M2'$. Using our data we have been able to show that these two traps have quite different energy level positions. The capture cross sections of $M1$, $M2$, and $M4$ were too large to measure directly.

Signatures of hole traps have been measured in a number of p-type samples and the same signatures have been found as minority carrier traps in n-type material, by using junction diodes and optical DLTS. Using the same techniques we have identified the "M" electron traps in p-type material.

Our experimental results are described in Secs. III–V: Sec. III gives a summary of the data in n- and p-type material, while Secs. IV and V concentrate on detailed measurements of emission rate, capture cross section, and the influence of growth conditions on the principal electron traps in n-type MBE GaAs. These results are discussed in detail in Secs. VI and VII. In Sec. VI we use our knowledge of the growth process and a comparison of trap signatures with those of other levels to make some tentative suggestions regarding the origin of the levels. Section VII gives a detailed analysis of the electronic properties of the levels including calculations of the true energy levels of $M2'$ and $M3$ and a discussion of the effect of all the levels in MBE GaAs on the minority carrier lifetime in p-type material.

II. EXPERIMENTAL DETAILS

Most of the n-type material for our DLTS experiments was grown in an ion-pumped Varian 360 growth system. Si-doped n^+ GaAs substrates were etched in 15:2:2 H_2SO_4:H_2O_2:H_2O prior to loading via the vacuum interlock, and then thermally cleaned in a flux of As_4. Films of 2-μm thickness were grown at a rate of 1 μm h^{-1}, using As_4:Ga flux ratios of 3:1, 5:1, and 7:1. The As_4 flux was always sufficient to maintain an As stable surface as determined by the RHEED pattern, and for a given flux ratio the As_4 and Ga fluxes were the same at each growth temperature. These ratios were determined by using a beam-monitoring ion gauge and correcting the pressure ratio for the difference in molecular masses and velocities, but not for the relative ionization efficiencies, which had not been determined for this gauge. Si and Sn were used for doping in the range mid 10^{15}–10^{17} cm^{-3}, at substrate temperatures T_g between 500 and 650 °C, as indicated by a thermocouple in contact with the back of the substrate mounting block. Some p-type material (Be-doped), Ge-doped n-type material and material for minority carrier trap measurements were grown in various home-built systems which were evacuated with liquid nitrogen-trapped diffusion pumps.

Schottky diode samples were prepared by alloying an evaporated AuSn back contact at 400 °C onto the n^+ substrate followed by evaporation of 0.5-mm-diam Al barriers on the epitaxial layer. Diodes were contacted by bonding, and we demonstrated, using a few samples, that this process had no effect on the DLTS spectra. With the exception of one layer grown at 300 °C, all the samples were grown at temperatures above 500 °C and variations in the back contact alloying schedule had no effect on the spectra. The diodes had ideality factors in the range 1.05–1.10 and series resistances of a few ohms. Details of all n-type samples are given in Table I.

Measurements of trap concentrations were done in a simple liquid nitrogen cooled cryostat. Data on trap signatures, profiles and capture cross sections were obtained using a temperature controlled continuous flow cryostat with a calibrated resistance thermometer embedded in the sample block. Temperature scans were done with a controlled sweep and with thermal hysteresis <0.2 K. DLTS measurements were made using a constant capacitance system which provided a direct readout of the amplitude of the voltage transient. The trap concentration N_t was calculated from the amplitude of the transient at the peak ΔV_0 using the equation

$$N_t = \frac{2\epsilon\epsilon_0}{e}\frac{\Delta V_0}{(x_2^2 - x_1^2)} \tag{1}$$

[see, for example, Eq. (10) of Ref. 5 with $t_1 = 0$ and $t_2 = \infty$]. The distances x_1 and x_2, shown in Fig. 1, are the depths below the surface where the trap level $E_t(x)$ crosses the Fermi level E_f during the trap filling period and trap emission period, respectively. These depths were calculated as

$$x_i = x_{di} - \lambda \quad (i = 1,2), \tag{2}$$

where x_{di} are the corresponding depletion depths obtained from the measured capacitance and λ is the distance from the depletion edge to the point where $E_t(x)$ crosses E_f:

TABLE I. Growth conditions and doping levels of the samples.

Layer number	As:Ga ratio	Growth temperature T_g(°C)	Dopant species	Carrier concentration n(cm^{-3})
139	2.5:1	650	Sn	2.5×10^{16}
140	2.4:1	625	Sn	7.0×10^{16}
152	7:1	650	Sn	5.0×10^{16}
153	5.7:1	630	Sn	6.0×10^{16}
154	7:1	610	Sn	1.2×10^{17}
155	7:1	500	Sn	5.5×10^{16}
156	7:1	550	Sn	1.3×10^{17}
158	5:1	600	Sn	5×10^{15}
176	5:1	650	Sn	3×10^{16}
177	5:1	550	Sn	1.3×10^{17}
184	5:1	550	Sn	7×10^{15}
187	5:1	520	Sn	1.4×10^{16}
189	3:1	650	Si	1×10^{16}
190	3:1	550	Si	1×10^{16}
464	8:1	550	Si	1.3×10^{16}
466	4.5:1	550	Sn	8.5×10^{16}

[This article is copyrighted as indicated in the article. Reuse of AIP content is subject to the terms at: http://scitation.aip.org/termsconditions. Downloaded to] IP: 133.1.198.126 On: Wed, 26 Nov 2014 07:07:39

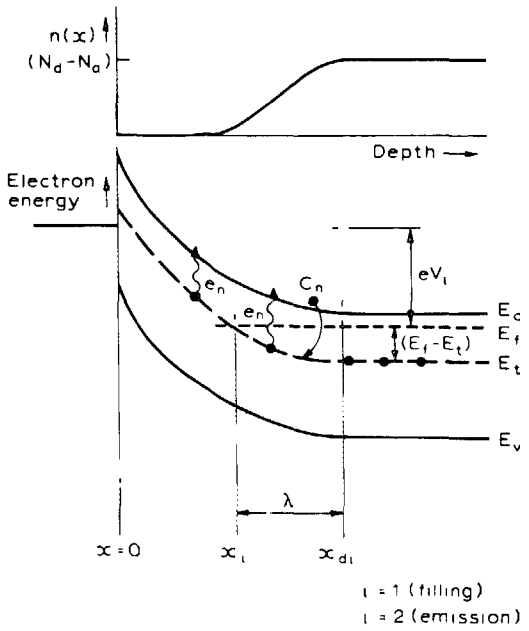

FIG. 1. Energy band diagram and free electron depth distribution $n(x)$for a Schottky barrier with band bending eV_i. The energies of the valence band edge, conduction band edge, Fermi level, and trap level are indicated by E_v, E_c, E_f, and E_t, respectively. The depletion depth is x_{di}, and the crossing of E_f and E_t occurs at x_i, where $i=1$ corresponds to the depth during the filling pulse and $i=2$ corresponds to the depth during the emission observation period. The electron emission and capture processes are indicated by e_n and c_n, respectively.

$$\lambda^2 = \frac{2\epsilon\epsilon_0}{e^2(N_d - N_a)}(E_f - E_t). \tag{3}$$

The net doping level $N_d - N_a$ was obtained from a room-temperature C-V measurement on each diode. $(E_f - E_t)$ is the separation between Fermi level and trap level in undepleted material. Since all the N_t measurements were taken from DLTS peaks above 100 K and the samples had $n \lesssim 10^{17}$ cm^{-3} the Fermi level position $(E_c - E_f)$ was calculated at each peak temperature assuming $n = (N_d - N_a)$ using Boltzmann statistics. The trap level $(E_c - E_t)$ required in Eq. (3) is the Gibbs free energy (G), not the measured activation energy of the emission rate $e_n(T)$ (see Sec. VII). We have been able to calculate the Gibbs free energy of $M2'$ and $M3$ from our capture cross sections results (Sec.VII A), and these values (given in Table V) have been used in Eq. (3) to calculate N_t using Eqs. (1) and (2). Such data are not available for $M1$, $M2$, and $M4$ and so we have used our measured activation energies E_{na} (Table II) as the best possible estimates of $(E_c - E_t)$. In Sec. VII B we estimate the lowest possible values for G (Table VI) and these imply the maximum systematic error in N_t to be an overestimate ranging from 6% for the deepest trap ($M4$) to about 2% for the shallowest ($M1$) when using the activation energy for $E_c - E_t$. Values for N_t were obtained from measurements on 3 or 4 diodes on each layer. The scatter in these measurements usually exceeds any random uncertainties arising from noise in ΔV_0 or errors due to subtraction of the tail of any adjacent peak, and usually this scatter is the error quoted for the results.

With the shallow depletion depths (~ 1 μm) used for some of our measurements the distance λ is a significant fraction of the total excursion of the depletion layer between filling and emptying $(x_{d2} - x_{d1})$ which defines the volume of material under observation in the emission period. Trap filling occurs in a time $\sim c_n^{-1} = (n\sigma_n v_{th})^{-1}$ where n is the local free electron concentration, σ_n the capture cross section, and v_{th} the thermal velocity of free electrons. The electron concentration decreases in the depletion region as depicted in Fig. 1 causing an increase in the time required to fill the traps in the region x_{d1} to x_1, and this incomplete trap filling can cause a significant reduction in the amplitude of the subsequent emission transient. Thus, for our N_t measurements the filling time t_f was set sufficiently long to fill all the traps up to x_1 and establish steady-state conditions. Since at x_1, $c_n(x_1) = e_n$ we usually set $t_f = e_n^{-1}$.

Capture cross-section measurements were made by applying a short and variable filling pulse, duration t_f, between the capacitance meter and the diode using an arrangement of field-effect transistor (FET) switches. The pulse was monitored with a probe at the leadthrough to the cryostat. The rise time was ~ 20 ns and the shortest pulses used were 60 ns. There was no ringing at the end of the pulse to cause additional trap filling. During the measurement of $\Delta V_0(t_f)$ the sample temperature was kept constant (within ± 0.15 K) at the DLTS peak.

III. GENERAL FEATURES OF RESULTS

Deep level spectra for three n-type Schottky barrier samples are shown in Fig. 2. At growth temperatures of 500 and 550 °C we observed three traps which can be identified with $M1$, $M3$, and $M4$ reported in Ref. 2. These three traps were always observed in material grown in this temperature range in five different growth systems, pumped with ion pumps or diffusion pumps; a fourth trap with a DLTS peak at 140 K tentatively ascribed to $M2$ was found under more restricted growth conditions. Further traps, manifesting themselves at 300 K and above on the DLTS scans as in Fig. 2, were detected in some samples and probably correspond to $M5$–8.[2] These peaks did not occur reproducibly, and in some instances they appeared to be associated with the near

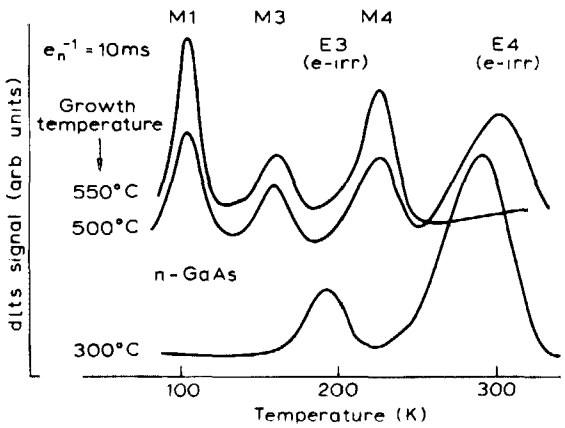

FIG. 2. DLTS spectra for n-type MBE GaAs grown at 300, 500, and 550 °C, for a reference time constant of 10 ms. The approximate locations of traps $E3$ and $E4$ reported for electron irradiated GaAs are also indicated (from Ref. 6).

[This article is copyrighted as indicated in the article. Reuse of AIP content is subject to the terms at: http://scitation.aip.org/termsconditions. Downloaded to] IP: 133.1.198.126 On: Wed, 26 Nov 2014 07:07:39

surface region of the material. At the significantly lower growth temperature of 300 °C, $M1$, $M2$, $M3$, and $M4$ did not occur but were replaced by the two peaks shown in the lower spectrum of Fig. 2, which may correspond to traps $E3$ and $E4$ in irradiated material.[3,6] Traps $M1$, $M3$, and $M4$ have been found in layers doped with Si, Ge, or Sn and $M2$ has been observed in Si- and Sn-doped layers. Ge-doped samples have not been grown under appropriate conditions for $M2$. Peaks $M1$, $M3$, and $M4$ have been detected in Be-doped p-type MBE layers by optical DLTS measurements.

A DLTS spectrum from a p-type sample is shown in Fig. 3, together with a spectrum from an Fe-diffused LPE sample obtained on the same equipment. The principal feature is a peak near 300 K which probably corresponds to the level $HL3$ ascribed to Fe in LPE GaAs.[7] (We measure $\sigma_p > 2\times10^{-17}$ cm^2, which is consistent with $\sigma_p \sim 10^{-16}$ cm^2 at 300 K in Ref. 8.) The peak at ~230 K labelled $HB4$ and $HL4$ (Ref. 7) probably corresponds to the level now ascribed to Cu.[9] Another level has been found close to $HL7$ previously reported in MBE material[7] but since this also appears in the LPE sample (Fig. 3) it is not unique to the MBE process. Figure 4 shows spectra obtained on an n-type sample by applying an injection pulse to a p^+-n junction diode, and by optical DLTS. Both spectra show evidence for the Cu hole trap near 200 K and the p^+-n diode shows evidence for the Fe related trap. We find that this trap is not easily excited in optical DLTS using a lamp of modest power and conclude that the optical cross section for excitation of an electron from the trap to the conduction band must be small. We find the same effect for the 300 K DLTS peak in the Fe diffused LPE sample of Fig. 3, and evidence for a very small optical cross section for the $HL3$(Fe) level has been reported by others.[10] We therefore feel confident in assigning the 300 K hole trap peak in MBE material to $HL3$(Fe).

We conclude that electron traps designated $M1$, $M3$, and $M4$, hole traps ascribed to Fe and Cu and the trap labelled $HL7$ are found in both n- and p-GaAs grown by MBE at about 550 °C. The traps labelled $M1$–$M4$ occur reproducibly in MBE GaAs and the rest of this paper is concerned with the behavior and properties of these centers in n-type material.

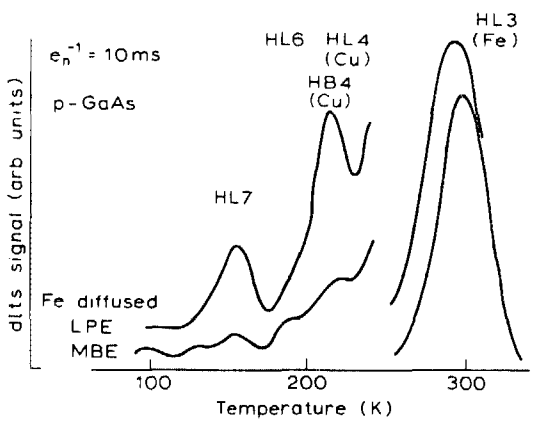

FIG. 3. DLTS spectra for p-type MBE GaAs and Fe-diffused LPE GaAs (time constant 10 ms). The locations of peaks due to traps $HL3$, $HL4$, $HL6$, $HL7$, and $HB4$ are taken from Ref. 7.

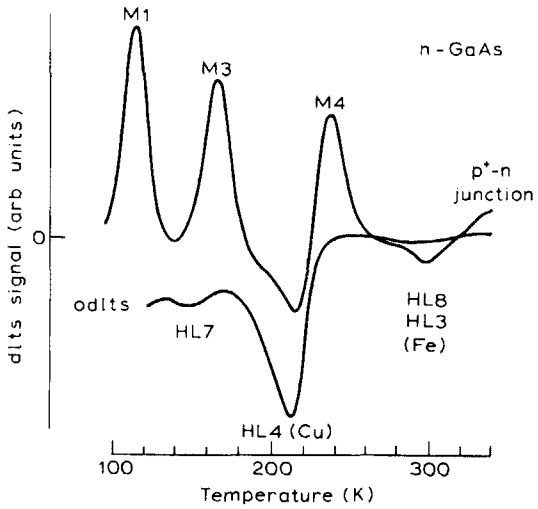

FIG. 4. DLTS spectra for n-type MBE GaAs obtained using an injection pulsed p^+-n junction and an optical DLTS (ODLTS) experiment. The negative-going peaks denote hole traps in the lower half of the band gap.

IV. EMISSION RATES AND CAPTURE CROSS SECTIONS

The temperature dependence of the emission rate e_n of electrons from a deep state to the conduction band can be written in the following empirical form[6]

$$e_n(T) = \langle v_{\rm th}\rangle N_c \sigma_{na} \exp\left(-\frac{E_{na}}{kT}\right), \tag{4}$$

where $\langle v_{\rm th}\rangle$ and N_c are the mean thermal velocity and effective density of states, respectively. The explicit temperature dependence of these two quantities is $T^{1/2}$ and $T^{3/2}$, respectively, so we write $\langle v_{\rm th}\rangle N_c = \gamma T^2$, where γ is dependent only upon the intrinsic properties of the material. An Arrhenius plot of T^2/e_n then represents the trap "signature" defined by an apparent cross section σ_{na} and an activation energy E_{na}.[6]

Signatures for the electron traps are shown in Fig. 5 for a variety of samples selected where possible for a low doping level. All were measured at low electric fields where we could detect no change in peak position with a change in applied bias. In all cases we observed lower emission rates than reported by Lang *et al.*[2] in higher doped samples and we ascribe this difference to enhancement of e_n by the electric field $\mathscr{E}$ in their samples. $M1$ is particularly sensitive: for a sample with $n = 8\times10^{15}$ cm^{-3}, we observed an increase in e_n by a factor 1.5 when the band bending was increased from 0.5 V ($\mathscr{E}_{\rm max} = 3.4\times10^4$ V cm^{-1}) to 3.0 V ($\mathscr{E}_{\rm max} = 8.3\times10^4$ V cm^{-1}). Thus for a sample with $n \sim 10^{17}$ cm^{-3} the resulting increase in $\mathscr{E}_{\rm max}$ at a given bias could easily account for an enhancement of e_n by a factor 2 or so.

For all the traps we observed small variations in the signature from sample to sample. A similar effect has been noted in VPE material.[11] Some samples were remeasured after 15 months and the results were the same within the experimental scatter. There is no obvious pattern to these variations. Thus, for $M1$, samples 158(Sn, $T_g = 600$ °C, $N_t = 4\times10^{13}$ cm^{-3}), 184(Sn, $T_g = 550$ °C, $N_t = 9.5\times10^{13}$ cm^{-3}), and 190(Si, $T_g = 550$ °C, $N_t = 1.7\times10^{14}$ cm^{-3}) have indistinguishable signatures; samples 464(Si, $T_g = 550$ °C, $N_t = 7.0\times10^{13}$ cm^{-3}) and 466(Sn, $T_g = 550$ °C, N_t

[This article is copyrighted as indicated in the article. Reuse of AIP content is subject to the terms at: http://scitation.aip.org/termsconditions. Downloaded to] IP: 133.1.198.126 On: Wed, 26 Nov 2014 07:07:39

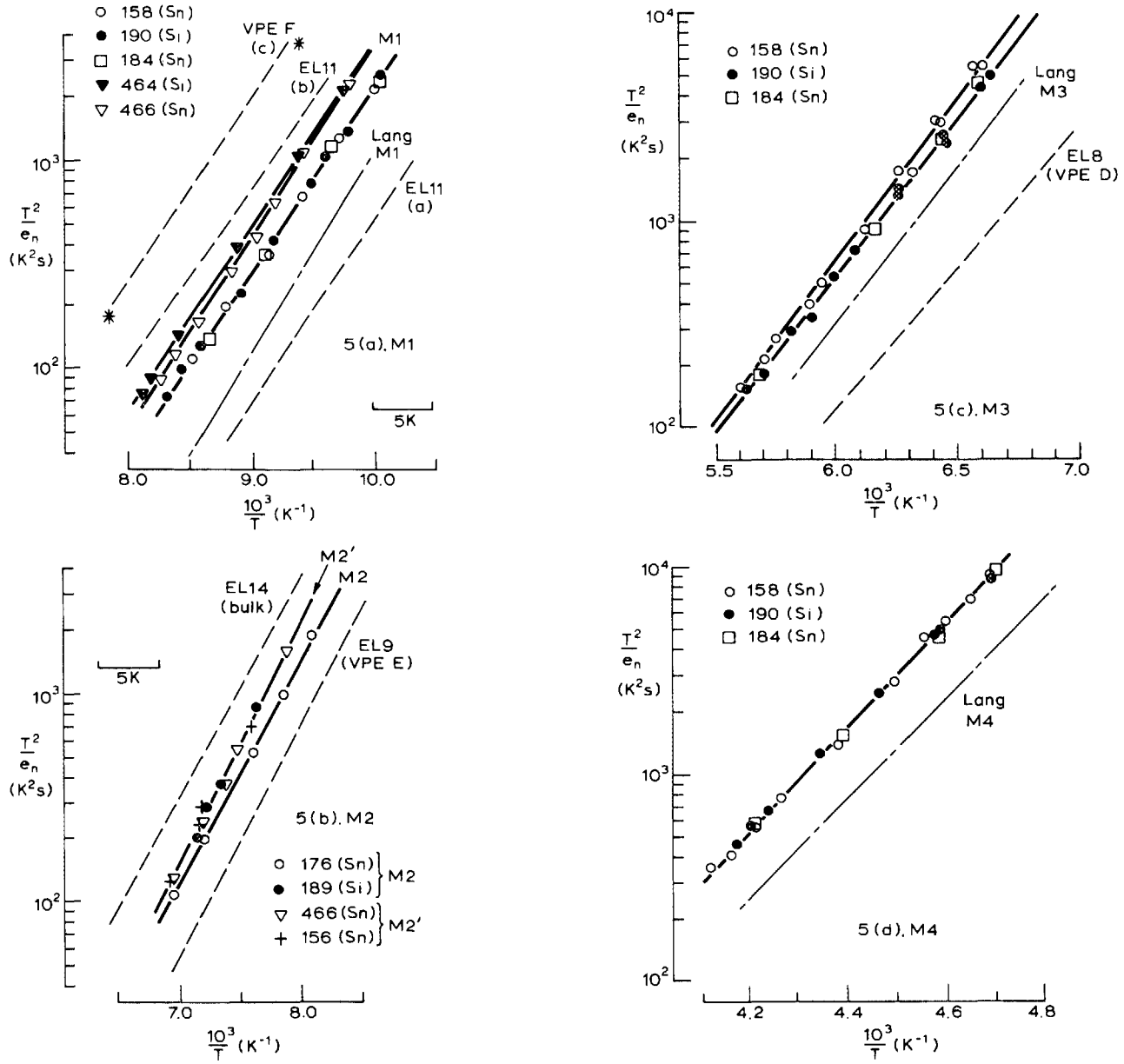

FIG. 5. Arrhenius plots of T^2/e_n for (a) M 1, (b) M 2 and M 2', (c) M 3, and (d) M 4, measured at low electric fields, and shown as experimental points with lines. Trap signatures for M 1, M 3, and M 4 measured by Lang *et al.*[2] and for the EL levels are taken from Ref. 6. On (a) EL 11 lines labelled (a) and (b) are taken from the figure and table of Ref. 6, respectively, and line (c) is for the trap labelled F in Fig. 2 of Ref. 11.

$= 4\times10^{13}$ cm^{-3}) grown two years later are different from the above but differ only slightly from each other. For M 3 there appears to be a small difference between 158(Sn) and 190(Si), equivalent to a peak shift of $\sim$1.3 K, whereas 184(Sn) and 190(Si) are in close agreement. For M 4 there is good agreement between all three samples. Samples 176(Sn) and 189(Si) both grown at 650 °C have different signatures for the 140 K peak whereas 466 and 156 grown at 550 °C have similar signatures. We conclude that these various differences do not correlate with the dopant species, and we have not found any obvious correlation with doping level n or trap concentration. In view of the influence of external electric fields on e_n we suggest that these variations may be due to the effect of electric fields of charged centers within the sample on the emission rate of the deep level center.

Such effects could be due to the dipole of donor-acceptor pairs, and therefore depend upon the acceptor concentration N_a. The moment (p) of this dipole will be weakest if the donor and acceptor are on nearest-neighbor sites ($\sim$2.5 Å), and the maximum possible spacing (r) between such a dipole and a deep level center is half the dipole spacing. In n-type material this is approximately half the average acceptor spacing if we assume all acceptors are paired with donors. From the 77 K mobility of a sample grown on an insulating substrate concurrently with sample 158 we estimate $N_a = 3.6\times10^{15}$ cm^{-3} so that for the circumstances detailed above $\mathscr{E} \sim 2p(4\pi\epsilon\epsilon_0 r^3)^{-1} \sim 1.6\times10^5$ V cm^{-1}. This field is certainly sufficient to influence the emission rate, and could well be larger for centers closer to a dipole pair. We therefore suggest that the differences between signatures of different samples is due to differences in the compensating acceptor concentration. The spread of trap signatures will be greatest

[This article is copyrighted as indicated in the article. Reuse of AIP content is subject to the terms at: http://scitation.aip.org/termsconditions. Downloaded to] IP: 133.1.198.126 On: Wed, 26 Nov 2014 07:07:39

TABLE II. Thermal activation energies E_{na} and prefactors σ_{na} of the signatures of traps $M1$, $M2'$, $M2$, $M3$, and $M4$. Data measured by Lang *et al.* (see Ref. 2) and Martin *et al.* (see Ref. 6) are also given, both taken from the compilation in Ref. 6.

Layer	T_g	Dopant	$M1$		140 K peak		$M3$		$M4$	
	(°C)		E_{na}(eV)	σ_{na}(cm^2)	E_{na}(eV)	σ_{na}(cm^2)	E_{na}(eV)	σ_{na}(cm^2)	E_{na}(eV)	σ_{na}(cm^2)
189	650	Si	...	...	0.22_7($M2$)	2.7×10^{-15}				
190	550	Si	0.17_7	1.6×10^{-15}			0.30_1	1.10×10^{-14}	0.49_2	2.1×10^{-13}
156	550	Sn	...	...	0.23_6($M2'$)	6.4×10^{-15}				
158	600	Sn	0.17_5	1.2×10^{-15}			0.31_4	2.3×10^{-14}	0.51_5	6.9×10^{-13}
176	650	Sn	...	...	0.22_0($M2$)	2.0×10^{-15}				
184	550	Sn	0.17_2	0.95×10^{-15}			0.30_6	1.5×10^{-14}	0.48_1	1.2×10^{-13}
464	550	Si	0.17_6	0.83×10^{-15}						
466	550	Sn	0.18_3	2.1×10^{-15}	0.23_9($M2'$)	8.3×10^{-15}				
Lang "EB" data			0.19	15×10^{-15}			0.30	1.7×10^{-14}	0.48	2.6×10^{-13}
Martin "EL" data			0.17	1.8×10^{-15}			0.30	0.72×10^{-14}	0.51	1.0×10^{-12}

for those deep level centers which have a strong field dependence, and furthermore such samples may show evidence for a distribution of emission rates corresponding to a statistical spread in the spacing r. Unfortunately we do not have compensation data on sufficient samples to test this hypothesis.

Values for E_{na} and σ_{na} obtained by least squares fitting are given in Table II. The greatest discrepancy with earlier data is for $M1$ which, as noted above, is very sensitive to electric field.

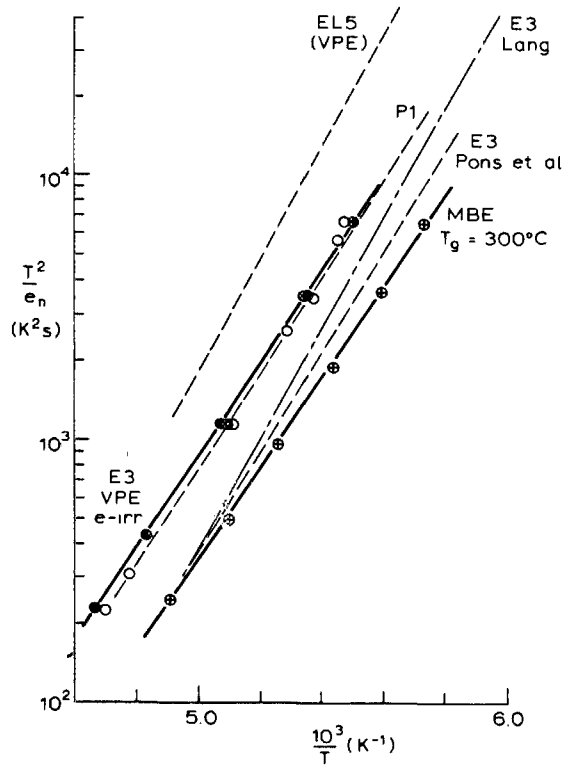

FIG. 6. Arrhenius plot of T^2/e_n for the 200 K peak observed in MBE GaAs grown at 300 °C. Experimental data for trap $E3$ in two samples of VPE material irradiated with electrons is shown, together with the signature of $E3$ measured by Lang and constructed from data in Ref. 6. Signatures are also given for $E3$ and $P1$ from Pons *et al.*,[20] and $EL5$ (VPE).[6]

We also investigated the signature of the peak near 200 K found in material grown at 300 °C, and this data is given in Fig. 6 and Table III. It has been suggested[3,12] that this trap may be the same entity as $E3$ in electron irradiated material, so we also measured the signature for this trap in two different irradiated vapor phase epitaxial layers (Fig. 6). The signature of the MBE trap does have the same slope as our irradiated material though a different preexponential factor. The values of n and N_t in the MBE sample are about 100 times greater than in our irradiated VPE layers. Due to the high value of n we were unable to obtain a direct measurement of σ_n in the MBE sample for comparison with our data on $E3$.

Figure 7 shows capture transients for $M1$, $M3$, and $M4$ on sample 190(Si); similar plots were obtained for sample 184(Sn). For $M1$ and $M4$ the capture process was so fast that we were only able to observe the slow capture process in the tail of the free electron distribution (see Fig. 1), despite attempts to reduce this by the use of a 0.5 V forward bias filling pulse. Using the point recorded at our shortest filling pulse (60 ns) we obtained the minimum values for σ_n given in Table IV. These results suggest that $M1$ and $M4$ have the largest cross sections, with $M3$ somewhat smaller. In sample 158, with a low doping level, we were able to deduce a capture cross section for $M3$ of $\sigma_n = 1.1\times10^{-16}$ cm^2 at 173 K. Cap-

TABLE III. Thermal activation energies E_{na}, prefactors σ_{na}, and measured capture cross sections (σ_n) for the 200 K peak in 300 °C grown MBE material and the $E3$ peak in electron irradiated VPE GaAs. Data for $E3$ originally due to Lang and Kimerling is taken from Ref. 6.

	E_{na}(eV)	σ_{na}(cm^2)	σ_n(cm^2)
MBE T_g = 300 °C	0.34_2	5.5×10^{-15}	$>2\times10^{-18}$ (200 K)
e-irr VPE1, $E3$	0.34_7	3.1×10^{-15}	
e-irr VPE2, $E3$	0.36_6	9.6×10^{-15}	0.85×10^{-16} (203 K)
Lang $E3$ (6)	0.41	2.6×10^{-13}	

[This article is copyrighted as indicated in the article. Reuse of AIP content is subject to the terms at: http://scitation.aip.org/termsconditions. Downloaded to] IP: 133.1.198.126 On: Wed, 26 Nov 2014 07:07:39

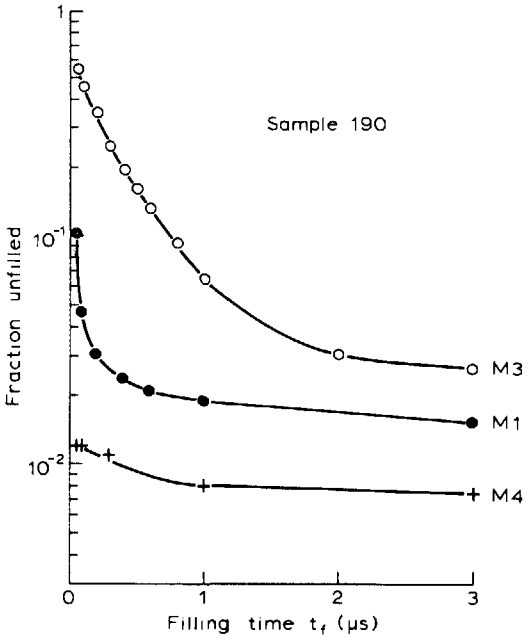

FIG. 7. Capture transients for $M1$, $M3$, and $M4$ in sample 190.

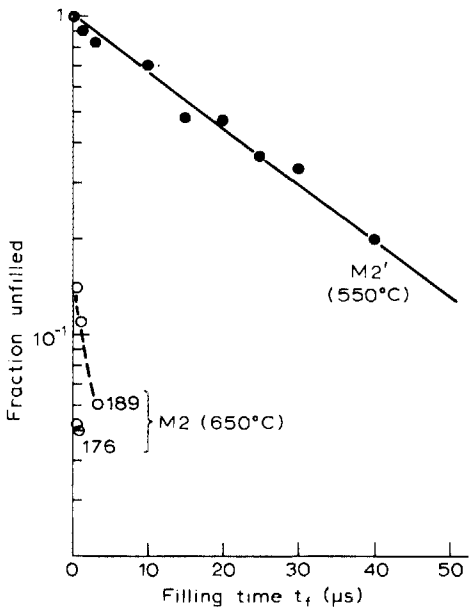

FIG. 8. Capture transient for $M2'$ measured in sample 156 grown at 550 °C. Data for $M2$ in samples 176 and 189 grown at 650 °C are shown on the same scale.

ture at $M1$ and $M4$ was still too fast to be measured in this sample. In 650 °C grown material the response of the 140 K peak was also dominated by slow tail capture and we deduced $\sigma_n > 4\times10^{-17}$ cm^2. We were able to observe clear exponential transients for this peak in material grown at 550 °C (Fig. 8) which gave $\sigma_n = 1\times10^{-20}$ cm^2. The large difference in capture cross section associated with the 140 K peak in 550 and 650 °C grown material indicates that different entities give rise to this peak in these two samples. On the basis of the growth behavior (Sec. V), we associate the peak in 650 °C material with $M2$ of Lang *et al.*[2] and thus in material grown at 550 °C we will designate the peak with low σ_n as $M2'$.

V. INFLUENCE OF GROWTH CONDITIONS

We have studied the effect of varying the growth temperature (T_g) between 500 and 650 °C using layers grown in a Varian 360 system with As:Ga ratios of about 3:1, 5:1, and 7:1. The properties of all these layers are summarized in Table I; the layers were deliberately grown in a random sequence as indicated by the layer numbers and layers 464 and 466 were grown two years after the original set.

Figure 9 shows the dependence of N_t on T_g for traps $M1$–4 for Sn-doped layers grown with As:Ga of 5:1. At 650 °C the traps $M1$, $M3$, and $M4$ were not observed above the detection limits shown in the figure (indicated by downward arrows); $M2$ was the dominant trap in this layer. As the growth temperature was reduced, N_t for $M1$ and $M4$ increased by about two decades in 100 °C, to a value of about 10^{15} cm^{-3} at 520 °C. $M3$ shows a similar increase in concentration down to 550 °C but N_t appears to decrease at lower growth temperatures. We note from Fig. 2 that the M levels are absent for $T_g \sim 300$ °C and so ultimately N_t must decrease for all these levels as the temperature is lowered further. A DLTS peak at 140 K was not detected in layers with $T_g = 630$ and 600 °C but at lower growth temperatures we observed a shoulder on the high-temperature side of the peak due to $M1$, as shown in Fig. 10. Although we were only able to measure σ_n of this trap directly in two 550 °C grown samples, the 140 K shoulder shown in Fig. 10 disappears when DLTS spectra are recorded with a short 1-μs filling pulse for all samples grown with $T_g < 600$ °C, and so by reference to Fig. 8 we infer that in these samples the 140 K peak is the trap we have designated $M2'$ and the data is labelled as such in Fig. 9. The $e_n(T)$ data for sample 189 (650 °C) looks

TABLE IV. Capture cross-section data (in cm^2) for the "M" levels in GaAs obtained at the DLTS peak temperatures given in parentheses for each level. The minimum values were estimated from the reduction in peak height at the shortest filling pulse available (60 ns). Measured values marked with an asterisk were obtained from exponential decay transients, such as Fig. 8.

Layer number	T_g(°C)	$M1$(116 K)	$M2'$(140 K)	$M2$(140 K)	$M3$(171 K)	$M4$(238 K)
176	650			$>10^{-17}$		
184	550	$>1.5\times10^{-16}$			$>5\times10^{-17}$	$>2\times10^{-16}$
189	650			$>4\times10^{-17}$		
190	550	$>1.4\times10^{-16}$			$>4\times10^{-17}$	$>2\times10^{-16}$
*156	550		1.0×10^{-20}			
*158	600				1.1×10^{-16}	
*466	550		1.6×10^{-20}			

[This article is copyrighted as indicated in the article. Reuse of AIP content is subject to the terms at: http://scitation.aip.org/termsconditions. Downloaded to] IP: 133.1.198.126 On: Wed, 26 Nov 2014 07:07:39

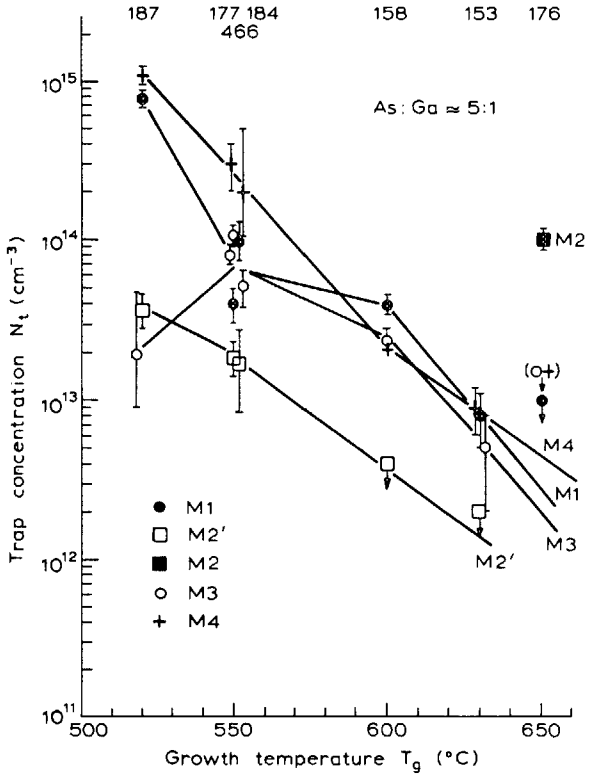

FIG. 9. Trap concentrations as a function of growth temperature for MBE GaAs samples grown with As:Ga = 5:1. The sample identification numbers are given across the top of the figure. Downward pointing arrows denote upper limits for N_t.

similar to that of 466 (550 °C) in Fig. 5, however, we did find that 189 has a large value of σ_n, similar to sample 176 (Table IV). The amplitude of the peak in sample 139 (650 °C) is not reduced by a 1-μs filling pulse. Thus in all 650 °C grown samples this center has a large σ_n, and we label this center $M2$. Figure 9 therefore shows that $N_t(M2)$ increases with increasing T_g at around $T_g = 650$ °C whereas $N_t(M2')$ decreases with increasing T_g in the range 520–600 °C.

Data for $N_t(T_g)$ for As:Ga ratios of 3:1 and 7:1 are shown in Fig. 11. The information from these samples is not as complete as that shown in Fig. 9 because in some samples the traps could not be detected.[13] Nevertheless the same features are apparent as in Fig. 9, principally a large decrease in

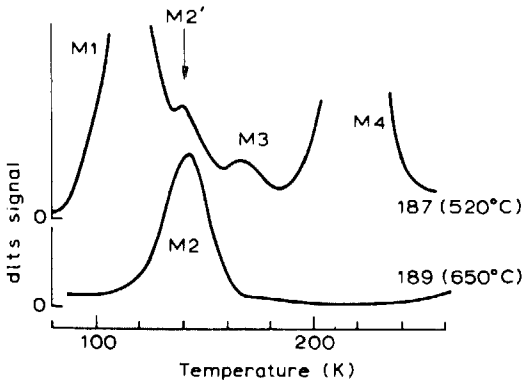

FIG. 10. DLTS spectra for samples grown at 520 and 650 °C, showing peak of $M2'$ on the shoulder of $M1$ at the lower growth temperature.

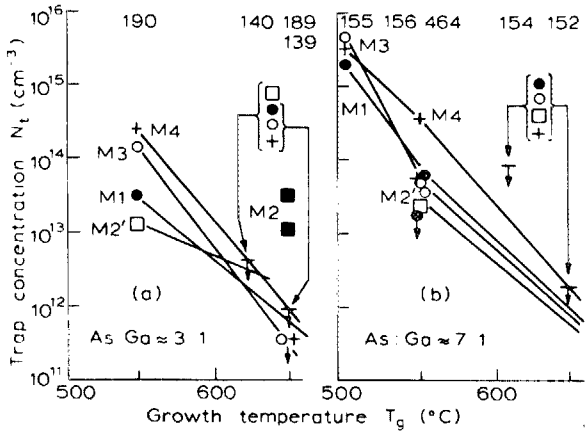

FIG. 11. Trap concentrations as functions of growth temperature for MBE samples with As:Ga ratios of (a) 3:1 and (b) 7:1. Sample identification numbers are given across the top of the figure. Downward pointing arrows denote upper limits for N_t.

N_t with increasing T_g. For an As:Ga ratio of 3:1, $M2$ was again dominant at $T_g = 650$ °C, and $M2'$ was observed at lower growth temperatures in samples 190 and 156. This trap may also be present in sample 155 but the peak was not visible on the broad shoulder of the large $M1$ peak.

Figure 12 shows N_t at $T_g = 550$ °C as a function of As:Ga ratio. In contrast to the effect of T_g, the variation of N_t was quite small though there is evidence that the concentrations of $M1$ and $M4$ decrease with increasing relative As flux while N_t for $M2'$ and $M3$ increases. The trap $M2$ in 650 °C material behaves differently, as shown in Fig. 13, with a marked decrease in N_t at a high As:Ga ratio. Since the trap labelled $M2$ by Lang *et al.*[2] was only observed for layers grown under Ga-rich conditions ($T_g \leqslant 610$ °C) we associated the center found in our 650 °C grown material with this trap.

We have measured the depth profiles of $M1$, $M3$, and $M4$ in two samples grown at different temperatures: 550 °C(190) and 600 °C(158). The samples were held at the DLTS peak temperature and the DLTS signal amplitude recorded as a function of the amplitude of the filling pulse V_1 at fixed reverse bias. The values of $N_t(x_1)$ were calculated from the differential form of Eq. (1),[5]

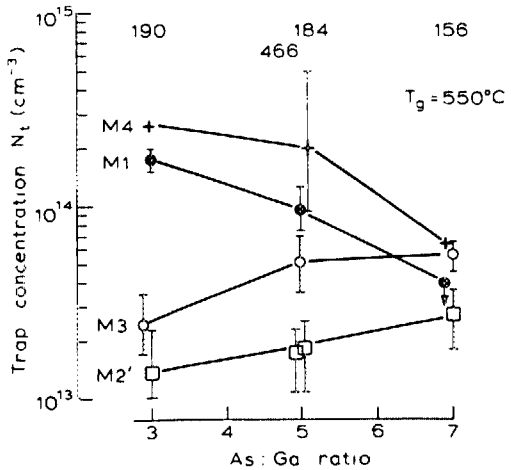

FIG. 12. Trap concentrations as function of As:Ga ratio for MBE GaAs grown at 550 °C.

[This article is copyrighted as indicated in the article. Reuse of AIP content is subject to the terms at: http://scitation.aip.org/termsconditions. Downloaded to] IP: 133.1.198.126 On: Wed, 26 Nov 2014 07:07:39

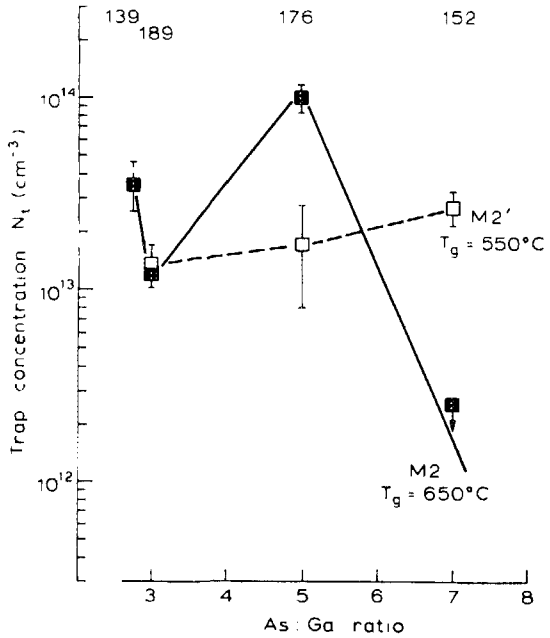

FIG. 13. Concentration of traps $M2$ and $M2'$ as a function of As:Ga ratio at growth temperatures of 650 and 550 °C, respectively. Samples grown at 650 °C are identified across the top of the figure.

$$N_t(x_1) = -\frac{\epsilon\epsilon_0}{e}\frac{1}{x_1}\frac{d\Delta V_0}{dx_1}. \tag{5}$$

The capacitance for each filling voltage was measured and x_1 calculated from Eqs. (2) and (3) as described in Sec. II. The profiles are shown in Fig. 14. In general these are all flat. The curvature near the surface may be due to errors in estimating λ, which will become apparent when x is small, while the curvature at the deep side of some profiles may be due to uncertainty in assessing the stray capacitance.

VI. NATURE OF DEEP LEVEL CENTERS IN MBE GaAs

In this section we will discuss the influence of the growth conditions on material quality in terms of our understanding of the growth process, and examine the possible relation between traps in MBE material and other samples of GaAs. We will then make some tentative suggestions on the origin of the "M" levels.

A. Influence of growth processes

The following model has been proposed to explain the surface processes controlling the growth of GaAs from beams of Ga and As_4 on (100) surfaces.[1,14] The As_4 molecules take part in a dissociative chemisorption process on adjacent Ga lattice sites. From an adjacent pair of As_4 molecules four As atoms are incorporated on lattice sites and four atoms desorb as an As_4 molecule. When the surface concentration of As_4 molecules is small the growth process is determined by the probability of pairs of As_4 molecules arriving at adjacent Ga sites and this in turn assumes that the As_4 molecules are mobile on the surface, whereas as the As_4 population is increased there is an increasing probability that an arriving molecule will find the adjacent site already occupied. At low growth temperatures (≤330 °C) the Ga adatom population

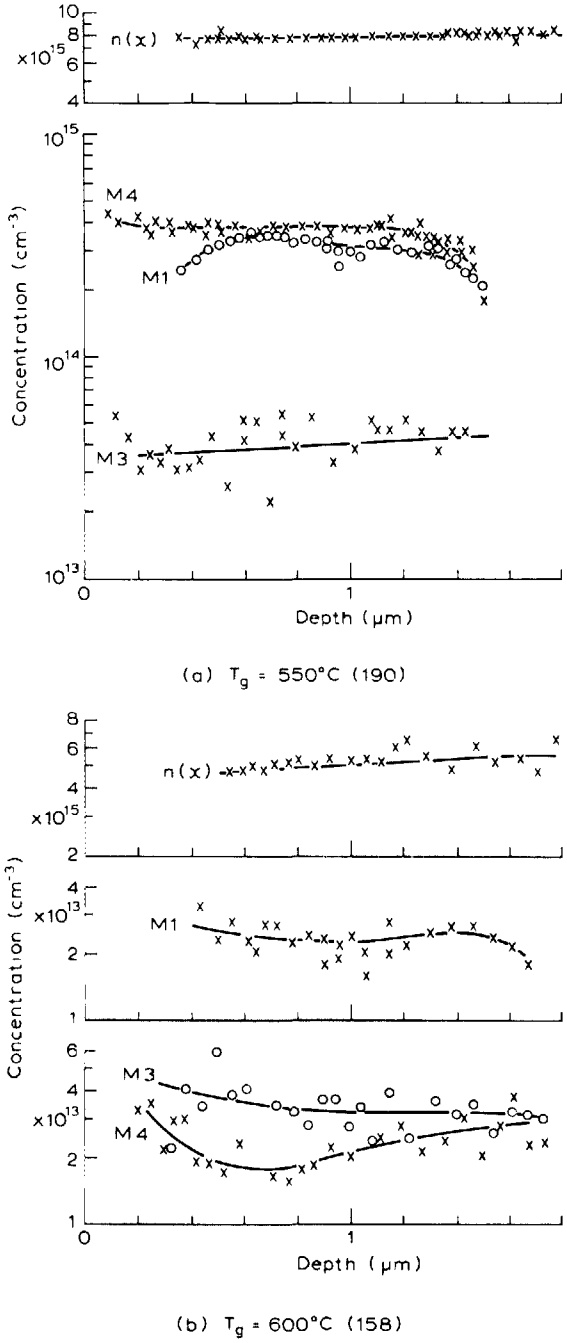

FIG. 14. Profiles of the carrier concentration (n) and trap concentrations for samples grown at (a) 550 °C and (b) 600 °C.

necessary for the sticking of As_4 is supplied by the molecular beam. When the Ga flux is less than the As flux, one As atom sticks for each Ga atom supplied, the surplus As reevaporating, whereas in the converse situation excess Ga is incorporated in the growing layer. At higher temperatures the growth process is fundamentally the same except that As_2 is thermally desorbed from the surface and further As must be supplied to maintain the surface stoichiometry.

The layers used in this work were grown at temperatures above 500 °C and with excess As to avoid the various difficulties which may arise from excess Ga incorporated in the films: the As_4 flux was such that the RHEED patterns indicated an As stable surface. Under these conditions we

[This article is copyrighted as indicated in the article. Reuse of AIP content is subject to the terms at: http://scitation.aip.org/termsconditions. Downloaded to] IP: 133.1.198.126 On: Wed, 26 Nov 2014 07:07:39

may expect the surface to contain some single isolated Ga sites where growth by the pairwise interaction is not possible thereby leaving groups of As vacancies as the layer grows. Growth from As_2 molecules occurs by a simple process of dissociative chemisorption[1,15] and since adjacent Ga sites are not now required, we would not expect such a large concentration of As vacancies in this case.

We have been unable to detect any correlation between the trap concentrations in our samples and the electron concentration or the donor dopant species. The "M" levels have also been detected in p-type material. The traps are not therefore associated with externally supplied donors, and by inference it is also unlikely that residual shallow donors are involved.

The concentrations of the centers found in material with $T_g < 600$ °C ($M1$, $M2'$, $M3$, and $M4$) all decrease with increasing T_g whereas $M2$ shows the opposite behavior (Fig. 9). Considering the first group of centers we note from Fig. 12 that these may be further subdivided according to their behavior with respect to the As:Ga ratio. As this ratio is increased traps $M2'$ and $M3$ have N_t increasing slightly whereas $M1$ and $M4$ decrease in concentration. This behavior suggests $M1$ and $M4$ may be related to As vacancies possibly created in the manner discussed above, and this is consistent with the reduction in N_t which we have found previously for these traps for growth using As_2 molecules.[4]

The growth temperature has a very strong effect on the values of N_t. The As vacancy concentration cannot therefore be the only factor controlling $N_t(M1, M4)$ because we would expect the increasing As desorption rate to give a higher concentration of unoccupied As surface sites at the higher growth temperature. Furthermore all four traps show a decrease in N_t with increasing T_g ($M3$ for $T_g > 550$ °C) irrespective of their dependence on flux ratio. We therefore consider three other factors which may control the formation of these deep level centers: (a) surface migration of As_4 molecules, (b) annealing in the bulk of the crystal during growth, and (c) residual impurity incorporation.

If the centers are complexes their formation may be controlled by the migration of surface As vacancies to achieve pairing with some extrinsic chemical species or other defect present on the surface in low concentration. However, if the dependence of N_t upon T_g is assumed to have an Arrhenius form (the data is not sufficiently accurate or extensive to determine whether this is so) then the data in Fig. 9 corresponds to an activation energy of approximately 1.4 eV. This is larger than the activation energy for surface migration of As_4 molecules of 0.24 eV (Ref. 14) and we conclude that this process is not controlling the formation of the deep level centers.

Another explanation of the effect of T_g is that after formation at the surface of the growing crystal the deep level centers anneal in the bulk during the continuing growth of material. It has been reported that the concentrations of $M1$ and $M4$ are reduced when MBE layers are capped with Si_3N_4 and annealed in the temperature range 500–600 °C (Ref. 16) but it is not known whether a similar annealing process occurs during growth. By annealing at 600 °C for 30 min the concentrations of $M1$ and $M4$ were reduced by a factor ~ 4 to about 1×10^{12} cm^{-3}.[16] If this represents the equilibrium concentration at this temperature we would expect similar N_t values in our samples, which have been grown for ~ 2 h, whereas Fig. 9 shows $N_t(M1, M3, M4) \sim 3 \times 10^{13}$ cm^{-3} at 600 °C. If equilibrium is not achieved in our samples, or in the event of incomplete annealing in the near surface regions of the crystal, then we would expect the unannealed fraction to depend on T_g because the growth times are similar. However, in this case, N_t should decrease with depth through the layer with the depth scale being equivalent to annealing time. This behavior is not observed in the profiles of Fig. 14 for layers grown at 550 and 600 °C. The only possibility permitted by this data is annealing within the time to grow ~ 0.3 μm, that is ~ 20 min, in which case N_t in the flat region must be the equilibrium concentration, though it is not in agreement with the value for capped samples.[16] Since our profiles are flat we believe that bulk annealing does not occur during growth. Furthermore, the activation energies for diffusion of As and Ga vacancies in the bulk of 4.0 and 2.1 eV, respectively,[17] are large compared with the activation energy of ~ 1.4 eV which we estimated above for $N_t(T_g)$. All this evidence suggests that bulk processes are not controlling the concentration of deep level centers in MBE material.

Finally we turn to the possible influence of impurity incorporation. Secondary Ion Mass Spectrometry (SIMS) measurements by Clegg *et al.*[18] have shown that the chemical concentrations of residual impurities in MBE GaAs samples decrease with increasing growth temperature, and concentrations of Mn, Fe, and Mg in particular fall by between one and two decades in the range 500–600 °C. Cu was not detected above the background limit of 2×10^{15} cm^{-3}. Although these layers are p type, some were grown in a Varian 360 system and we have detected traps ascribed to Fe and Cu in our n-type layers. The chemical concentrations of Mn, Fe, and Mg given in Ref. 18 are greater than the values of $N_t(M1, M2', M3, M4)$ measured in our layers. It is therefore possible that these impurities are incorporated both on "simple" (substitutional?) sites, which we suppose to be represented by hole traps $HL4$ and $HL3$, and also in the form of defect-impurity complexes unique to the MBE growth process. We do not believe the M levels are other charge states of the "simple" centers because they should then be observed in other kinds of GaAs. The impurities involved in these complexes must be common to the majority of MBE growth systems, and in Ref. 18 the heaters of high-temperature evaporation sources such as those for Al, Ga, and Si were identified as the possible origin of contaminants. The differences in N_t between different growth systems then represent differences in detailed design of the source assembly whereas the dependence of N_t upon T_g in a particular system is due to the decrease in impurity content with increasing T_g shown by the SIMS data.[18]

The behavior of trap $M2$ in material grown above 600 °C would appear to be simpler than the centers in material grown at lower temperatures. The marked decrease of N_t with increasing As:Ga ratio and the increase with increasing T_g both suggest this trap may be a defect or defect complex involving As vacancies.

The influence of growth conditions on the electron

[This article is copyrighted as indicated in the article. Reuse of AIP content is subject to the terms at: http://scitation.aip.org/termsconditions. Downloaded to] IP: 133.1.198.126 On: Wed, 26 Nov 2014 07:07:39

traps in MBE material may be summarized as follows. We have shown that the concentrations of the principal deep states are not controlled by bulk annealing processes. The rapid decrease of N_t with T_g for $M1$, $M2'$, $M3$, and $M4$ is the opposite behavior to that expected if the concentrations are determined only by the surface As vacancy concentration. We therefore suggest, by comparison with SIMS data, that this behavior is related to the growth temperature dependence of the incorporation of residual impurities, although traps $M1$ and $M4$ may also involve As vacancies. Trap $M2$ shows a rapid increase in concentration with T_g above 600 °C and a decrease in N_t with increasing As:Ga ratio from which we infer that this center is probably a defect complex incorporating As vacancies.

B. Trap signatures

Since our trap signatures obtained at low electric fields are different from earlier data[2] we should compare them with data for traps in other samples of GaAs. There are very few comments on the elimination of field enhancement in other published work so we have selected data from Ref. (6) where the doping level was reported to be low and hence the enhancement likely to be small.

The signature of $M1$ lies near EL 11 (VPE) though there seems some confusion over the signature of this latter trap. The signature plotted for EL 11 in the figure of Ref. 6, shown as line (a) in our Fig. 5(a), differs from the line (b) defined by the parameters in the table of that reference, while the original data (Ref. 11, Table II) gives another line (c). The data for trap F [$= EL$ 11 (Ref. 6)] read from Fig. 2 of Ref. 11 gives the star points in Fig. 5(a). In measurements on fourteen VPE layers we always observed a trap fitting line (a) but no traps in the vicinity of lines (b) or (c). Thus there is original experimental data for traps in VPE material with signatures defined by lines (a) and (c), but these are both significantly different from $M1$, which suggests that the latter is unique to MBE material. The data supporting lines (a) and (c) was obtained on low doped samples so the electric field effect should be small.

Traps $M2$ and $M2'$ have signatures close to EL 9 (VPE) and EL 14 (bulk) [Fig. 5(b)], though the latter may have been measured in highly doped material and therefore be displaced to the low-temperature side of its true position. The signatures for $M3$ [Fig. 5(c)] and EL 8 (VPE) are sufficiently different for these traps to be different entities, and there are no other traps reported with signatures in the vicinity of $M4$ [Fig. 5(d)].

Using our low field data we conclude that $M1$, $M3$, and $M4$ are unique to MBE growth whereas $M2$ and/or $M2'$ may be identified with EL 9. None of these traps may be identified with traps in irradiated material.

In Fig. 6 we compare the signature of the DLTS peak near 200 K found in 300 °C grown material with data for the irradiation-induced center $E3$. The data for $E3$ of Lang and Kimerling,[19] Pons *et al.*,[20] and our own measurements all differ. Our data for $E3$ lies very close to the signature for $P1$ (Ref. 20) which is found after annealing irradiated material at temperatures above 200 °C (our samples were irradiated after alloying the back contact). Data for MBE material lies close to the signature for $E3$ as measured in Ref. 20 using layers with doping levels ranging between 1 and 6×10^{16} cm^{-3}. This is surprising since we would expect $E3$ to anneal in the bulk at the growth temperature of 300 °C so that we should be more likely to observe trap $P1$. The identification of the MBE trap with $E3$ is not conclusively proven and, in view of the annealing temperature of $E3$, is perhaps unlikely.

C. Possible origin of the levels

In the intermediate growth temperature range 500–600 °C we suggest that $M1$ and $M4$ are impurity-defect complexes possibly involving As vacancies (V_{As}). The formation of these centers is controlled by the impurity incorporation process, which is strongly temperature dependent. Traps $M2'$ and $M3$ are probably also impurity related, though of a different nature to $M1$ and $M4$ by virtue of their different response to an increase in relative As flux. At growth temperatures above 600 °C these centers are not observed and this could be due to the very low concentration of impurities incorporated in the crystal. However, since the number of surface As vacancies is increasing with growth temperature, the formation of defect complexes, such as a divacancy, becomes more probable than a V_{As}-impurity complex. We suggest that $M2$ is such a defect complex, and this assignment is supported by the decrease of $N_t(M2)$ with increasing As:Ga ratio. The formation of such centers may not be unique to MBE growth and the possible identification of $M2$ with EL 9 in VPE material is therefore quite reasonable. At low growth temperatures the deep level centers may be related to antisite defects[12] because of the increased difficulty in breaking the bonds between the two As_4 molecules involved in the pairwise interaction,[14] resulting in incorporation of As on Ga sites. Pons and Bourgoin have shown that $E3$ in irradiated material is related to a defect formed by displacement of the As sublattice[21] and Pons[22] has further suggested that in its most stable form the interstitial As displaces a Ga atom to form a complex incorporating an antisite defect. However, the question remains whether such a defect can be associated with the 200 K DLTS peak in MBE material and whether it remains stable at 300 °C under MBE growth conditions.

VII. ELECTRONIC PROPERTIES OF THE TRAPS

The emission rate of electrons from a trap with capture cross section σ_n is given by[23,24]

$$e_n(T) = \sigma_n \langle v_{th} \rangle N_c \exp\left(-\frac{G(T)}{kT}\right). \tag{6}$$

The energy level of the trap with respect to the conduction band edge ($E_c - E_t$) is the temperature dependent Gibbs free energy of the center $G(T)$ (Ref. 25) given by the thermodynamic identity

$$G(T) = H - T\Delta S \tag{7}$$

where H is an enthalpy and ΔS is the entropy change on emission or capture of an electron. If we allow for a temperature dependence of σ_n of the form[6,26]

$$\sigma_n = \sigma_\infty \exp\left(-\frac{E_\sigma}{kT}\right), \tag{8}$$

[This article is copyrighted as indicated in the article. Reuse of AIP content is subject to the terms at: http://scitation.aip.org/termsconditions. Downloaded to] IP: 133.1.198.126 On: Wed, 26 Nov 2014 07:07:39

then $e_n(T)$ takes the form

$$e_n(T) = \langle v_{th} \rangle N_c \sigma_\infty \exp\left(\frac{\Delta S}{k}\right) \exp\left(-\frac{H + E_\sigma}{kT}\right). \quad (9)$$

We can again write $\langle v_{th} \rangle N_c = \gamma T^2$, then comparison with Eq. (4) shows that the parameters defining the trap signature are given by

$$E_{na} = H + E_\sigma \quad (10)$$

and

$$\sigma_{na} = \sigma_\infty \exp\left(\frac{\Delta S}{k}\right). \quad (11)$$

A. Energy levels of $M2'$ and $M3$

Using the values of σ_n measured for $M2'$ and $M3$ (Table IV) we can calculate the energy levels of these traps at the temperature of the σ_n measurement using Eq. (6), giving values of ~ 0.080 and 0.236 eV, respectively (Table V). These free energies are lower than values of E_{na} given in Table II, in the case of $M2'$ by a large amount. This difference may be due to both the entropy term in Eq. (7) and E_σ in Eq. (10). Accordingly we have estimated E_σ by measuring the temperature dependence of σ_n over a temperature range of about 15 K. Measurements over a wider range were not possible because of interference from other peaks. These measurements gave $E_\sigma = 0.12$ and 0.04 eV for $M2'$ and $M3$, respectively. With these data we calculated the enthalpy (H) for each trap using Eq. (10), and with values for the free energy derived above from Eq. (6) we used Eq. (7) to obtain the entropy values $\Delta S/k$ given in Table V. Also shown is the effect of an increase by a factor 2 in σ_n, and the effect of an uncertainty of ± 0.02 eV in E_σ.

The entropy change ΔS is due to both changes in the electronic configuration of the defect and changes in the lattice vibrational entropy (ΔS_{vib}). In general for deep states these two contributions are coupled by the electron-vibronic interaction and only in rather restricted circumstances, specified in Ref. 24, can ΔS be expressed as separate terms, one due to the electronic degeneracy of the defect state and the other due to the change in cohesive character of the defect brought about by a change in occupancy of the bonding states. For the special case of an antibonding donor state, such as a simple donor, this separation is permissible and we would expect $\Delta S_{vib} = 0$ and an electronic contribution of $\Delta S/k = \ln(g'/g^0) = \ln 1/2 = -0.69$,[27] where g^0 and g' are the electronic degeneracies of the occupied and unoccupied states, respectively. If however the electron occupies a bonding state of the defect, the lattice entropy change may be estimated from the entropy change occurring when a free carrier is excited from the valence to conduction bands.[24,27] This is given by the entropy obtained from the temperature dependence of the band gap. The data of Thurmond[28] gives $\Delta S_{vib}/k = 3.5$ and 4.4 at the temperatures of measurement of $M2'$ and $M3$, respectively. Although this calculation is rather simplified and the effect of electronic degeneracy has been neglected, it does indicate that the values of $\Delta S/k$ obtained from analysis of our experimental data for $M2'$ and $M3$ are physically reasonable (Table V). The values of $\Delta S/k$ show that these states are certainly not simple donors, and are more likely to be bonding in character.

Another way of viewing the data is to regard ΔS and ΔS_{vib} as the parameters describing the temperature dependence of the energy level $(E_c - E_t)$ and the band gap $(E_c - E_v)$, respectively. The data in Table V shows that ΔS and ΔS_{vib} are similar so that $(E_t - E_v)$ is approximately temperature independent. Both energy levels are therefore pinned to the valance band, despite the fact that they are located in the upper half of the band gap, and are therefore made up of bonding states as concluded above.

Rather than dwelling on a detailed interpretation of this data the point we wish to stress is that for both $M2'$ and $M3$ our values for E_{na} and σ_n and our estimates of E_σ lead to physically reasonable values of ΔS. The measurements are therefore consistent and the energy level values $(E_c - E_t) = G(T)$ derived from Eq. (6) must be substantially correct. The consequences of erroneously equating the energy level with the activation energy E_{na} are well demonstrated by the data for $M2'$. In this case neglect of E_σ gives $\Delta S/k = 13.3$ which is physically very unlikely.

Because $\Delta S \neq 0$ the values of $(E_c - E_t)\,(= G)$ are temperature dependent and the data in Table V only applies at the specified temperatures. If we assume that H and ΔS are temperature independent (unlikely for ΔS), Eq. (7) gives $(E_c - E_t) = 0.036$ and 0.208 eV at 300 K for $M2'$ and $M3$, respectively. Although $M2'$ is quite shallow its concentration is too small to affect the interpretation of room temperature Hall data in our samples. In attempting to intentionally dope GaAs with Fe during MBE growth at 540 °C, Covington *et al.*[29] measured a net donor concentration of $\sim 10^{17}$ cm^{-3} which they were not able to associate directly with Fe. Recalling our suggestion that the M levels are impurity-defect complexes characteristic of MBE, it is interesting to specu-

TABLE V. Properties of traps $M2'$ and $M3$ at the specified temperatures. The Gibbs free energy G is calculated from Eq. (6) and the enthalpy H is obtained from Eq. (10) using the measured values given for E_σ. The entropy change ΔS is calculated from Eq. (7). The effects of doubling σ_n and an error of ± 0.02 eV in E_σ are also given. The values for ΔS_{vib} are calculated from the temperature dependence of the band gap of GaAs (see Ref. 28).

Trap	Sample	T(K)	σ_n(cm^2)	G(eV) $= (E_c - E_t)$	E_{na}(eV)	E_σ(eV)	H(eV)	$\Delta S/k$ (expt)	$\Delta S_{vib}/k$ (calc)
$M2'$	156	140	1.0×10^{-20}	0.073					
	466	139	1.6×10^{-20}	0.080	0.239	0.12 ± 0.02	0.119 ± 0.02	$3.2^{1.6}_{4.9}$	3.5
			(3.2×10^{-20})	(0.089)				(2.5)	
$M3$	158	173	1.1×10^{-16}	0.236	0.314	0.04 ± 0.02	0.274 ± 0.02	$2.5^{1.2}_{3.9}$	4.4
			(2.2×10^{-16})	(0.247)				(1.83)	

[This article is copyrighted as indicated in the article. Reuse of AIP content is subject to the terms at: http://scitation.aip.org/termsconditions. Downloaded to] IP: 133.1.198.126 On: Wed, 26 Nov 2014 07:07:39

late that $M2'$ is an Fe-defect complex and responsible for this donor behavior. As the Fe flux was increased the compensation of this n-type doping also increased[29] suggesting that Fe is increasingly incorporated on the HL 3 site which is taken to be acceptorlike. Their photoluminescence spectra provide evidence for Fe on a Ga site in MBE GaAs, which we take to be the hole trap HL 3.

B. Energy levels of $M1$, $M2$, and $M4$

We were not able to measure σ_n directly for $M1$, $M2$, and $M4$ and so it is not possible to calculate values for the energy level using Eq. (6). However, it is possible to obtain upper and lower limits to G. For a given value of e_n at a temperature T, Eq. (6) shows that the maximum and minimum values of σ_n correspond to the maximum and minimum values of G. The minimum values of σ_n are given by our capture transient data, listed in Table IV. Using these values in Eq. (6) we obtained the minimum values for G given in Table VI, at the temperatures specified. The maximum value of σ_n is approximately σ_{na} since $\sigma_n < \sigma_\infty$ [Eq. (8)] and $\sigma_\infty \leqslant \sigma_{na}$ [Eq. (11)] and so the corresponding maximum value of G is E_{na}, the slope of the Arrhenius plot of $e_n(T)$. Values of E_{na} from Table II are reproduced in Table VI.

Equations (7) and (10) may be combined to exhibit the relation between $G(T)$ and E_{na}

$$G(T) = E_{na} - E_\sigma - T\Delta S. \tag{12}$$

The maximum value of $G(T) = E_{na}$ therefore implies that $(E_\sigma + T\Delta S) = 0$. No negative values of E_σ have been reported for electron capture in GaAs (Ref. 30, Fig. 7) and so if we make the reasonable assumptions that both E_σ and ΔS are positive then $G(T) = E_{na}$ implies that both E_σ and ΔS are zero. $G^{\max}$ is therefore approximately temperature independent. In the event of $G(T)$ taking its minimum value then $(E_\sigma + T\Delta S)$ takes the maximum value given by $E_{na} - G(T)$ and this is the maximum possible value which $T\Delta S$ may take in the event of $E_\sigma = 0$. This value is given in Table VI. Notice that the corresponding values of $S^{\max}$ are physically reasonable for both $M1$ and $M2$ so that a large value of E_σ is not necessary to reconcile the properties of these traps. By contrast we would predict a large value for E_σ for $M4$, or a large capture cross section approaching our value of σ_{na}.

Using these arguments the possible behavior of the energy levels of $M1$, $M2$, and $M4$ are illustrated in Fig. 15. The energies are plotted as positive quantities below the conduction band edge as functions of temperature. The maximum separation is $(E_c - E_t) = G^{\max} = E_{na}$, which is temperature independent. The minimum values are plotted using the values of $G(T)$ obtained from σ_n estimates, given in Table VI. These are extrapolated to 300 K using a maximum slope given by values of $T\Delta S^{\max}$ in the table. Equation (7) shows that $G(T)$ linearly extrapolated back to $T = 0$ is the enthalpy H which in the above limit of $E_\sigma = 0$ is equal to E_{na} as apparent in the figure. In the event of $E_\sigma > 0$ the values of H and ΔS will be reduced such that the values of $(E_c - E_t)$ above the temperature of the $G(T)$ point are increased. If the true value of σ_n is greater than our limiting values then $(E_c - E_t)$ will again be increased so that solid lines in Fig. 15 delineate the boundaries of the values of $(E_c - E_t)$. We have also plotted the actual values of $G(T)$ which we obtained for $M2'$ and $M3$, again assuming ΔS is temperature independent.

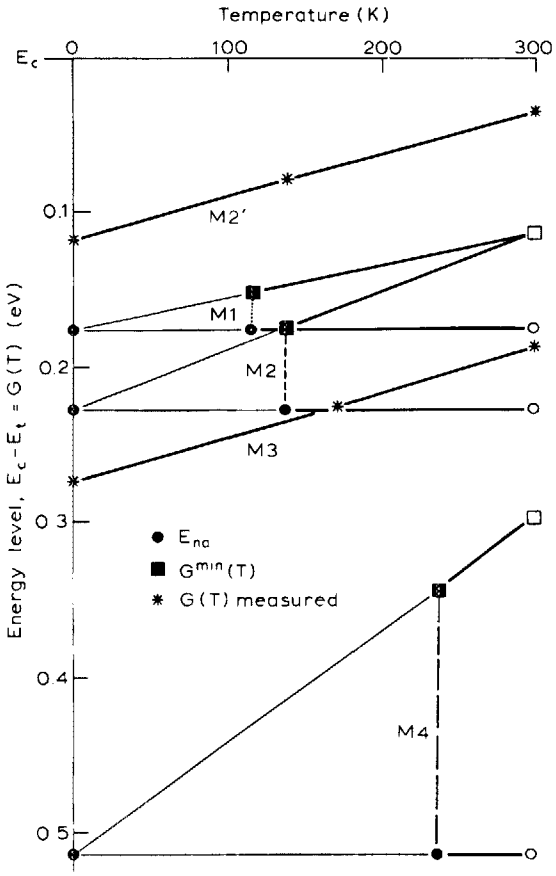

FIG. 15. Energy levels of deep states in MBE GaAs measured with respect to the conduction band edge E_c as functions of temperature. Limiting values are obtained from E_{na}(●) in Table II and $\sigma_n^{\min}$(■) in Table IV using Eq. (6). Measured values are given for $M2'$ and $M3$(*) from Table V. Extrapolations to room temperature are performed as described in the text.

TABLE VI. Minimum values for the energy levels $(E_c - E_t)$ of $M1$, $M2$, and $M4$ at the specified temperatures calculated from the minimum values of σ_n (Table IV) using Eq. (6), and the maximum values defined by E_{na} (Table II). The values of $T\Delta S$ and $\Delta S/k$ are given for $G(T) = G^{\min}(T)$ and $E_\sigma = 0$.

Deep state:	$M1$	$M2$	$M4$
Temperature T(K):	116	139	238
$G^{\min}(T)$, from σ_n(eV)	0.153	0.174	0.343
$G^{\max}(T)$, $= E_{na}$(eV)	0.177	0.227	0.515
$T\Delta S^{\max} = E_{na} - G^{\min}$(eV)	0.024	0.053	0.172
$\Delta S^{\max}$	2.4	4.4	8.3

The importance of the information in Fig. 15 is that it shows that at both the temperature of measurement (140 K) and room temperature the energy levels of $M2$ and $M2'$ are quite different. The fortuitous coincidence of their DLTS peaks arises because of the large contribution of E_σ to the thermal activation energy of the shallower trap $M2'$. The figure also indicates the range of energies where we may expect these traps to manifest themselves in a room-temperature experiment.

[This article is copyrighted as indicated in the article. Reuse of AIP content is subject to the terms at: http://scitation.aip.org/termsconditions. Downloaded to] IP: 133.1.198.126 On: Wed, 26 Nov 2014 07:07:39

C. Capture cross sections

Measured values of the capture cross sections of $M2'$ and $M3$ are given in Table IV. From our limited measurements of σ_n as functions of temperature we obtained $\sigma_\infty = 3.6^{(19)}_{(0.7)} \times 10^{-16}$ cm^2 and $1.6^{(6)}_{(0.4)} \times 10^{-15}$ cm^2 for $M2'$ and $M3$, respectively. These results are in reasonable agreement with the theory of electron capture by multiphonon emission of Henry and Lang which gives $\sigma_\infty \sim 6 \times 10^{-15}$ cm^2 (Ref. 26), and with the other experimental values of σ_∞ in GaAs shown in Ref. 26. The values of σ_n extrapolated to 300 K are 3.4×10^{-18} and 3.4×10^{-16} cm^2 for $M2'$ and $M3$, respectively.

For traps $M1$, $M2$, and $M4$ we were unable to measure σ_n from the filling transients. Following the discussion of Sec. VII B it follows that upper limits to the capture cross sections are given by the values for σ_{na} in Table II, and lower limits are given by our data in Table IV.

We can use this data to estimate the possible contribution of these traps to the low injection ($\Delta n \ll p$) minority carrier lifetime of electrons in p-GaAs, given by $\tau_{nr} \sim (N_t \sigma_n v_{th})^{-1}$. To assess the relative contribution of the traps we have calculated values of τ_{nr} in Table VII for $N_t = 10^{14}$ cm^{-3}, which is typical of our material at ~ 600 °C (Fig. 9). We have also included data for the hole traps ascribed to Fe and Cu, also present in our material. The radiative lifetime in GaAs with $p \sim 10^{16}$ cm^{-3} is about 3×10^{-7} s so the data in the table shows that only $M1$, $M2$, and $M4$ are likely to have a significant effect. The inequality signs in the table are reminders that the values of τ_{nr} have been obtained from maximum values of σ_n given by σ_{na} which apply at all temperatures. The data in Fig. 7 shows that $\sigma_n(M4) > \sigma_n(M1)$, and in fact the true value of $\sigma_n(M4)$ would have to be almost three orders of magnitude smaller than $\sigma_{na}(M4)$ for $M1$ to dominate over $M4$. Since $M1$ and $M4$ usually occur in similar concentrations we therefore expect recombination via $M4$ to be the dominant nonradiative path.

Experimental data have been published for τ_{nr} in p-GaAs obtained from analysis of external photoluminescence efficiency measurements on Be-doped material grown in a Varian 360 system under As-rich conditions.[31] We have calculated values of τ_{nr} corresponding to four of the samples used in this work having $p \sim 3$–5×10^{16} cm^{-3} and T_g increasing from 480 to 660 °C, assuming that the trap concentrations as functions of T_g are given by our data in Fig. 9 with extrapolations to 480 °C. In accordance with the discussion above we have considered only $M4$ and $M2$: Table VIII gives the values of N_t and the $N_t \sigma_n$ products for each trap, together with final values for τ_{nr} and the measured values from Ref. 31. Clearly our data for $N_t(T_g)$ accounts for the increase of τ_{nr} with increasing T_g and the numerical agreement at all but the lowest temperatures is surprisingly good. The point at $T_g = 480$ °C represents a large extrapolation of N_t in Fig. 9 which may well be an overestimate because we know that at lower values of T_g the trap $M4$ is not present. Although we have used an upper limit for $\sigma_n(M4)$ rather than the true measured value we see that the $(N_t \sigma_n)$ product correctly accounts for both the qualitative temperature dependence of τ_{nr} and its magnitude. In the temperature range up to ~ 620 °C, $M1$ has the next largest value of σ_n but from the maximum value of σ_n given by $\sigma_{na}(M1)$ in Table II the concentration of $M1$ would have to be at least 2.6×10^{16} cm^{-3} to account for the value of τ_{nr} (580 °C) in Table VIII. Thus, we suggest that the temperature dependence and value of τ_{nr} in MBE p-GaAs grown in the temperature range 500–660 °C can be accounted for by recombination at the growth induced defects $M4$ and $M2$. On this model we would predict a maximum of τ_{nr} at around 670 °C with a decrease at higher growth temperatures due to the increasing concentration of $M2$. Further data is needed to confirm these suggestions.

VIII. CONCLUSIONS

Both n- and p-type GaAs layers grown by MBE in the region of 550 °C contain hole traps ascribed to Fe and Cu and native electron traps labelled $M1$, $M3$, and $M4$. A further trap $M2'$ has been observed in n-type material. The depth profiles of $M1$, $M3$, and $M4$ are flat and we argue that there is therefore no bulk annealing of these centers during growth so that the trap concentrations are determined by surface processes. In n-type material the concentrations of $M1$, $M2'$, $M3$, and $M4$ show only a weak dependence on As:Ga ratio but decrease by about two decades for an increase in substrate temperature from 500 to 600 °C. The latter observation suggests the deep level centers are not simple As-vacancy related defects, and furthermore the temperature dependence is not consistent with a process controlled by the surface migration of As atoms. By comparison with published data for the chemical concentrations of residual impurities in MBE GaAs we suggest that these deep level centers are defect-impurity complexes, with temperature dependent concentrations controlled by the incorporation of the impurity. Traps $M1$ and $M4$ show similar behavior with the flux ratio and may be related. Electron capture cross-

TABLE VII. Estimates of the low-injection nonradiative lifetime τ_{nr} of electrons in p-type GaAs due to recombination via deep states in MBE GaAs at 300 K and for a concentration of each state of $N_t = 10^{14}$ cm^{-3}.

Deep state	σ_{na}(cm^2)	σ_n(300 K) (cm^2)	$\tau_{nr} = (N_t \sigma_n v_{th})^{-1}$(ns)
$M1$	1.6×10^{-15}		>180
$M2'$		3.4×10^{-18}	6.7×10^4
$M2$	2.7×10^{-15}		> 84
$M3$		3.4×10^{-16}	670
$M4$	6.9×10^{-13}		0.33
HB 3,*HL* 3(Fe)		$\sim 10^{-19}$[a]	230×10^6
HB 4,*HL* 4(Cu)		$\sim 10^{-20}$[a]	230×10^6

[a] Reference 8.

[This article is copyrighted as indicated in the abstract. Reuse of AIP content is subject to the terms at: http://scitation.aip.org/termsconditions. Downloaded to] IP: 133.1.198.126 On: Wed, 26 Nov 2014 07:07:39

TABLE VIII. Values of τ_{nr} calculated as a function of T_g using $N_t(T_g)$ from Fig. 9 and values of σ_n in Table VII. The measured values are taken from Ref. 31.

	T_g	$M2$		$M4$		τ_{nr}(s)	τ_{nr}(s)
Sample	(°C)	$N_t(\text{cm}^{-3})$	$N_t\sigma_n(\text{cm}^{-1})$	$N_t(\text{cm}^{-3})$	$N_t\sigma_n(\text{cm}^{-1})$	calc	meas
MBE76	480			5×10^{15}	3.4×10^{3}	6.6×10^{-12}	1×10^{-10}
MBE71	580			6×10^{13}	4.1×10^{1}	5.5×10^{-10}	5.2×10^{-10}
MBE77	620			1×10^{13}	6.9	3.3×10^{-9}	$>1.8\times10^{-9}$
MBE89	660	3×10^{14}	0.81	2×10^{12}	1.38	1.0×10^{-8}	$>1.7\times10^{-8}$

section measurements have shown that two different entities $M2'$ and $M2$ give rise to DLTS peaks near 140 K with activation energy ~ 0.23 eV. A trap with large cross section, which we identify with $M2$ of Lang *et al.*, is observed at a growth temperature of 650 °C. In contrast to the other levels, its concentration increases with growth temperature above 600 °C and, consistent with a decrease with increasing As:Ga ratio, we suggest that this center is related to As vacancies. In material grown at 550 °C we observe the peak at 140 K of a trap labelled $M2'$, with a cross section of 10^{-20} cm^2 which exhibits the growth characteristics noted above. Comparisons of emission rate signatures obtained at low electric fields with published data suggest that only $M2$ and $M2'$ may possibly be identified with traps in other kinds of GaAs. The evidence for the proposed identification of the 200 K peak in 300 °C grown material with $E3$ in irradiated material is not yet convincing. From measurements of capture cross section we deduce energy levels for $M2'$ and $M3$ of $(E_c - E_t) = 0.08$ eV (139 K) and 0.23_6 eV (173 K), respectively. The entropy factors suggest that these levels are both associated with bonding states. Capture cross sections of the other traps were too large to be measured, though we deduce that $\sigma_n(M4) > \sigma_n(M1)$. From the estimated limiting values we have shown that $M2$ must have an energy level at least 0.17_4 eV from the conduction band, significantly deeper than $M2'$ despite their similar signatures. We suggest that recombination at $M4$ limits the low injection minority carrier lifetime in low doped p-type GaAs grown in the temperature range up to about 600 °C with an increasing contribution from $M2$ at higher growth temperatures.

ACKNOWLEDGMENTS

We thank J. Bicknell for devising the trap filling system for capture cross-section measurements, A. D. C. Grassie for help with the optical DLTS measurements. D. W. Palmer (University of Sussex) for the loan of one electron-irradiated VPE sample, G. M. Martin (LEP Paris) for the Fe-diffused sample, and S. D. Brotherton, G. J. Parker, and J. P. Stagg for helpful discussions. Additional MBE samples were provided by J. S. Roberts and C. T. Foxon. We especially thank P. J. Hulyer for his skillful fabrication of the samples and measurement of the characteristics of the diodes.

[1] C. T. Foxon and B. A. Joyce, "Fundamental aspects of molecular beam epitaxy," *Current Topics in Materials Science*, edited by E. Kaldis (North-Holland, Amsterdam, 1981), Vol. 7, pp. 1–68.
[2] D. V. Lang, A. Y. Cho, A. C. Gossard, M. Ilegems, and W. Wiegmann, J. Appl. Phys. **47**, 2558 (1976).
[3] R. A. Stall, C. E. C. Wood, P. D. Kirchner, and L. F. Eastman, Electron. Lett. **16**, 171 (1980).
[4] J. H. Neave, P. Blood, and B. A. Joyce, Appl. Phys. Lett. **36**, 311 (1980).
[5] N. M. Johnson, D. J. Bartelink, R. B. Gold, and J. F. Gibbons, J. Appl. Phys. **50**, 4828 (1979).
[6] G. M. Martin, A. Mitonneau, and A. Mircea, Electron. Lett. **13**, 191 (1977).
[7] A. Mitonneau, G. M. Martin, and A. Mircea, Electron. Lett. **13**, 666 (1977).
[8] D. V. Lang and R. A. Logan, J. Electron. Mater. **4**, 1053 (1975).
[9] V. Kumar and L-Å. Ledebo, J. Appl. Phys. **52**, 4866 (1981).
[10] A. Mitonneau, G. M. Martin, and A. Mircea, Inst. Phys. Conf. Ser. **33a**, 73 (1977); M. Kleverman, P. Omling, L-Å. Ledebo, and H. G. Grimmeiss, J. Appl. Phys. **54**, 814 (1983).
[11] A. Mircea and A. Mitonneau, Appl. Phys. **8**, 15 (1975).
[12] C. E. C. Wood, J. Woodcock, and J. J. Harris, Inst. Phys. Conf. Ser. **45**, 28 (1979).
[13] The detection limit is set primarily by the sensitivity of the DLTS system, which was about $\Delta V_0/V \sim 3\times10^{-5}$. Since $N_t/n \sim \Delta V_0/V$ the ultimate limit is determined by the doping level (n) of each sample. In practice the limit is increased by excess noise on the DLTS trace and so the limits indicated in the figures are calculated for each sample from the noise level at the appropriate temperature using Eq. (1). In some instances the ultimate limit was attained: for example, in sample 152 [Fig. 11(b)] we calculated $N_t < 2.5\times10^{12}$ cm^{-3} for $n = 5\times10^{16}$ cm^{-3}.
[14] C. T. Foxon and B. A. Joyce, Surf. Sci. **64**, 293 (1977).
[15] C. T. Foxon and B. A. Joyce, Surf. Sci. **50**, 434 (1975).
[16] D. S. Day, J. D. Oberstar, T. J. Drummond, H. Morkoç, A. Y. Cho, and B. G. Streetman, J. Electron. Mater. **10**, 445 (1981).
[17] S. Y. Chiang and G. L. Pearson, J. Appl. Phys. **46**, 2986 (1975).
[18] J. B. Clegg, C. T. Foxon, and G. Weimann, J. Appl. Phys. **53**, 4518 (1982).
[19] D. V. Lang and L. C. Kimerling, Inst. Phys. Conf. Ser. **23**, 581 (1975).
[20] D. Pons, A. Mircea, A. Mitonneau, and G. M. Martin, Inst. Phys. Conf. Ser. **46**, 352 (1979).
[21] D. Pons and J. Bourgoin, Phys. Rev. Lett. **47**, 1293 (1981).
[22] D. Pons, Physica **116B**, 388 (1983).
[23] O. Engström and A. Alm, Solid State Electron. **21**, 1571 (1978).
[24] J. E. Lowther, J. Phys. C **13**, 3681 (1980).
[25] J. A. van Vechten and C. D. Thurmond, Phys. Rev. B **14**, 3539 (1976).
[26] C. H. Henry and D. V. Lang, Phys. Rev. B **15**, 989 (1977).
[27] S. D. Brotherton and J. E. Lowther, Phys. Rev. Lett. **44**, 606 (1980).
[28] C. D. Thurmond, J. Electrochem. Soc. **122**, 1133 (1975).
[29] D. W. Covington, J. Comas, and P. W. Yu, Appl. Phys. Lett. **37**, 1094 (1980).
[30] A. Mitonneau, A. Mircea, G. M. Martin, and D. Pons, Rev. Phys. Appl. **14**, 853 (1979).
[31] G. B. Scott, G. Duggan, P. Dawson, and G. Weimann, J. Appl. Phys. **52**, 6888 (1981). The Varian 360 samples used for the SIMS work in Ref. 18 are the same as those used in this reference and the same as three of the samples quoted in Table VIII.

[This article is copyrighted as indicated in the article. Reuse of AIP content is subject to the terms at: http://scitation.aip.org/termsconditions. Downloaded to] IP: 133.1.198.126 On: Wed, 26 Nov 2014 07:07:39